Available online at www.sciencedirect.com

ScienceDirect

Procedia CIRP 82 (2019) 383–388

www.elsevier.com/locate/procedia

17th CIRP Conference on Modelling of Machining Operations

Thermal characterization methodology for dry finishing turning of SAF 2507 stainless steel based on finite element simulations and surrogate models

Rodolfo Franchi[a], Michele Giannuzzi[a,], Gabriele Papadia[a,]

[a]*Department of Engineering for Innovation, University of Salento, via per Monteroni, 73010 Lecce, Italy*

Abstract

This paper addresses the numerical thermal characterization of a 3D turning process of a SAF 2507 stainless steel. A thermographic test campaign was conducted to measure the temperature distribution at the tool-workpiece interface. The campaign was accommodated by means of a L_{18} fractional factorial design of experiment. The 3D turning process was simulated using the software TWS Advantedge. The heat transfer numerical coefficients were calibrated against experimental measures to obtain temperature values as accurate as possible. A statistical methodology framework was adopted to study the dependence of the coefficients from the machining parameters. A heat transfer surrogate model was then built and next experimentally validated.

Peer-review under responsibility of the scientific committee of The 17th CIRP Conference on Modelling of Machining Operations

Keywords: Finite element method (FEM); Calibration; High strength steel

1. Introduction

The SAF 2507 (also known as ASTM A995 gr.5a, EN 1.4410) is a high-performance Super-Duplex Stainless Steel (S-DSS), usually applied in strong, aggressive environments with high mechanical loads. It is characterized by excellent resistance to stress corrosion cracking (SCC) in environments with chlorine, excellent resistance to pitting and interstitial corrosion, high mechanical strength, and good weldability. The physical properties giving superior mechanical performances are the same which make these alloys difficult to cut. The main difficulties encountered in the machining of high-strength alloys are mainly due to heat generation. This phenomenon is linked to the high forces required to deform the material, to the friction at the tool-workpiece interface, and to the low heat transfer coefficient. Indeed, during machining operations, the heat at the clearance face and the rake face of the insert is generally very high. The result is a sharp increase in temperature of the insert, which implies an increase in flank wear and consequently a considerable reduction in the tool life. It is therefore essential to measure the temperatures in order to explain the physics of the tool wear process; this can be done in several ways and one of the most successful is the thermography. Besides the experimental approach, also the numerical one can be employed to understand the process deeply. In some machining simulations, as addressed in Yen *et al.* [2], large values of Heat Transfer Coefficient (HTC) are used since the thermal exchange at the interface is considered 'perfect', but this is, most of the time, misleading. As addressed in Filice *et al.* [1], a value of H = 1000 (kW/m^2K) has been identified giving satisfactory numerical results compared with the experimental values. In Xie *et al.* [3] to realize the thermal steady state in the whole tool, heat transfer analysis is performed with ABAQUS/Standard employing a Python user subroutine. The subroutine launches heat transfer analysis job automatically every time the cutting process variables at steady state are needed. Despite the effectiveness of the predictions, the way of doing seems to be quite cumbersome. In Umbrello *et al.* [4], a model for the HTC prediction has been built based on the value of normal pressure and the average temperature on the tool-chip interface. The results showed that the HTC increases when the two parameters increase. In the same work, the HTC behavior was investigated based on the cutting parameters. In Burte *et al.* [5] the HTC for various types of metal machining (hot forging, metal machining, ...) has been measured. In Childs *et al.* [6], the HTC was analyzed taking into account the role of the coolant during a mild steel machining. From the articles above, it is clear that the role

E-mail addresses: michele.giannuzzi@unisalento.it (Michele Giannuzzi)., gabriele.papadia@unisalento.it (Gabriele Papadia).

2212-8271
Peer-review under responsibility of the scientific committee of The 17th CIRP Conference on Modelling of Machining Operations
10.1016/j.procir.2019.04.155

of the heat transfer requires a more in-depth investigation. In the paper hereunder, the authors have built an empirical model of the heat transfer coefficient, in the sense of statistics, to be included in a numerical machining model. The empiric relationship between the numerical heat transfer coefficient and the machining parameters has been developed through a statistical methodological framework. The cutting parameters considered in this study were three - cutting speed, feed rate and depth of cut -. Each of them set at three levels. Since it was impractical to vary one factor at a time and since it was not economically convenient to test all combinations of factors, the selection of runs has been crucial. Hence, a statistically well-designed experiment was used where the number of tests was minimized making the empirical approach quite efficient.

Summing up, in this research an experimental infrared campaign was carried out to collect data of temperatures during dry finish turning of SAF 2507 stainless steel, see Table 1. The experimental campaign was accommodated in a $L_{18} - 2 \cdot 3^{7-5}$ fractional factorial design. The temperatures acquired were used to calibrate and validate a 3D finite element model built in TWS Advantedge software. Specifically, a statistical methodology framework was used to analyze the dependencies between the numerical heat transfer coefficients and the cutting factors, and next to develop the surrogate model. The equation is then used to predict the heat transfer coefficient of some other experimental points in order to validate the numerical model. The rheological model of the SAF 2507 stainless steel has been previously calibrated and validated in Franchi *et al.* [10].

In specific, the description of the experiment is in section 2, the discussion on methods is in section 3, and the results are addressed in section 4. The conclusions are reported in section 5.

2. Experiment

The workpiece used for the experiment was a rotating disk worked out by a hydraulic pump used in the Oil & Gas sector. The tool direction was perpendicular to the spindle axis, see Figure 1. The tool used was an 80° rhombic insert, commercially known as Sandvik Coromant CNMG643 2025 Grade Carbide Turning Insert TiCN/A (ANSI definition). The tool holder ensured a negative rake angle equal to -6°. The experimental activities were carried out on a double-pallet Carnaghi Lathe (TNA22) with a SINUMERIK 840D CNC system, with a maximum power of the spindle of 67 (kW), and a maximum rotational speed of 430 RPM.

A FLIR SC640 thermal infrared camera with a resolution of 640 x 480 pixels was used to acquire the apparent temperatures. The camera is equipped with a microbolometer detector that is constantly open to incoming radiation, no integration time is available. In order to follow the temperature variations, frequencies between 3 and 10 Hz have been selected. The detector was calibrated based on the theory of the black body. It was positioned approximately 30 cm away from the workpiece, pointing at the interface tool-workpiece area, see Figure 2. The selected frame has been chosen in such a way that the disk, the two sides of the insert and the chip can be viewed simultaneously. For each test, both the workpiece and the insert were painted with high-emission paint, as shown in Figure 1.

Table 1. Workpiece material properties of SAF 2507 stainless steel

Chemical composition %weight								
C	Cr	Ni	Mo	Mn	Si	N	P	S
0.015	24.92	6.91	4.06	0.75	0.25	0.3	0.021	0.007
Mechanical properties								
Yield strength (MPa)								579
Tensile (MPa)								826
Hardness (BHN)								232
Elongation(%)								40

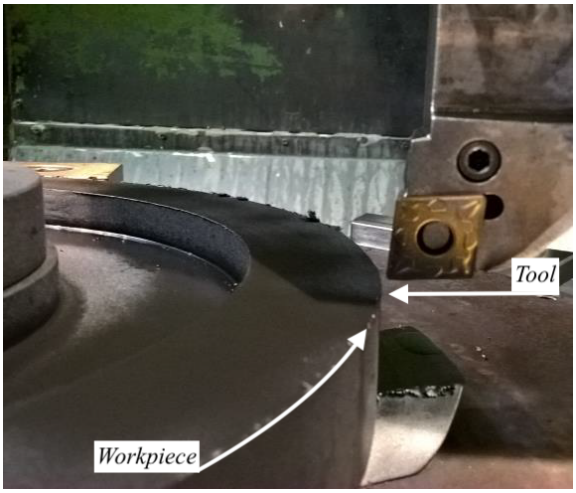

Fig. 1. The experiment setup used to measure the radiant temperature of the tool–workpiece interface. The arrows explain the directions.

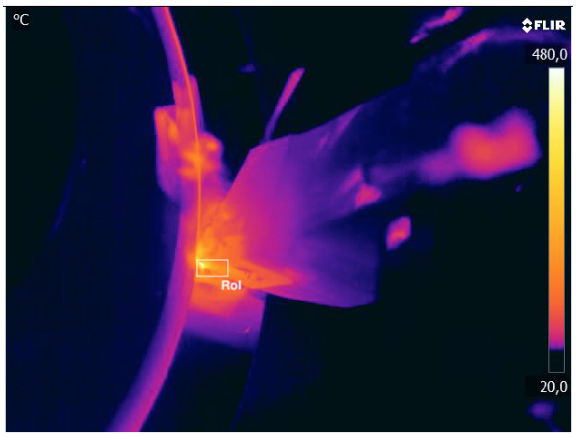

Fig. 2. An infrared screenshot extracted from a video during an experimental test. The tool-workpiece interface is the zone where the higher temperature is reached. In white the Region of Interest (the tool-workpiece interface area) is shown.

Table 2. Cutting parameters and level of variations

Factor	Identification	Levels
Cutting speed (m/min)	S	60, 80, 100
Feed Rate (mm/rev)	F	0.2, 0.3, 0.4
Depth of Cut (mm)	D	0.5, 1.0, 1.5

3. Methods

3.1. The design of the experiment and the infrared testing

As said afore, this study aims to analyse the influence of the cutting parameters, see Table 2, on the heat transfer coefficient obtained from machining simulations. In the beginning, the whole campaign should have examined twenty-seven possible combinations (i.e., a full factorial design); but given the limited number of inserts, an experiment with fewer experimental points has been designed. In fact a screening investigation based on an orthogonal array with 18 runs has been used; specifically, it was employed a $L_{18} - 2 \cdot 3^{7-5}$ fractional factorial design with no replications. An experimental plan of this kind can be created with the free open-source R package DoE.base, as addressed in Gromping [7]. A fractional factorial design is needed to systematically minimize the number of runs while maximizing the information to be obtained. Often, strong interactions among many factors are unlikely, so a right design places sample points in the way that multiple factor interactions are lumped together (in statistical terms, confounded). The appropriate choice of points allows a loss of information to be both controlled and predictable. Hence, the design has been optimized concerning the low-order effects: all main effects are orthogonal to each other, and confounding between main effects and two-factor interactions was minimized. The degrees of freedom of this experimental plan are 17.

Hence, three cutting parameters, see Table 2, were screened in a randomized experimental orthogonal design with limited confounding. The experimental design, in non-coded values, is given in Table 3. Abbreviations are as follows: F, feed rate (mm/rev); S, cutting speed (m/min); D, depth of cut (mm). In Figure 3 a mosaic plot for a triple of design factors shows a mild confounding between main effects and two-factor interactions, indeed any level combination of the factors "feed" and "speed" does not determine the level of factor "depth" completely. The cutting conditions were chosen based on technical raccomandations; each cut was performed in dry working conditions. The temperature measures acquired during the experimental campaign are shown in the column T_{exp} of Table 3. These values were calculated as the average of the values in the stationary portion of the time-temperature curves. The Region of Interest where the true temperature was extracted is shown in Figure 2

3.2. Finite element thermal characterization

The 3D turning operations of SAF 2507 were simulated using the TWS Advantedge finite element software. The numerical model has been calibrated using the Johnson-Cook (JC) law Johnson *et al.* [9]. The JC law describes the non-linear work-

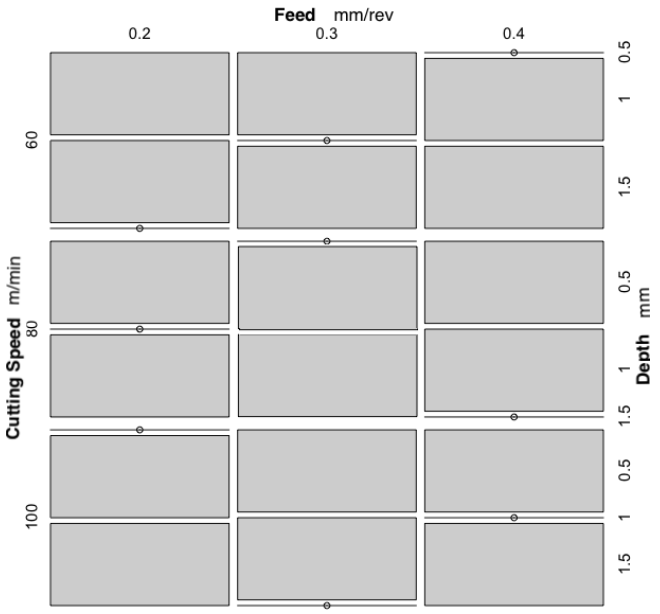

Fig. 3. Mosaic plot for a triple of design factors. The behavior of the split indicates the severity of confounding in the triple of columns. A flat line in the mosaic plot instead of a proper rectangle indicates that the respective combination does not occur at all.

Table 3. Experimental campaign: a no-replicated fractional factorial DoE with 17 Degrees of Freedom

Experimental campaign					Numerical		
#	S	F	D	T_{exp}	HTC	T_{num}	$\|\Delta\|$ %
1	60	0.2	1.0	342	350	347	1.5
2	80	0.4	0.5	346	610	325	6.0
3	60	0.4	1.0	426	150	424	0.5
4	100	0.2	1.0	362	660	364	0.5
5	100	0.3	0.5	346	910	325	6.0
6	60	0.3	0.5	292	600	292	0.0
7	60	0.2	0.5	265	800	264	0.4
8	60	0.3	1.5	439	100	414	5.7
9	100	0.4	0.5	366	720	346	5.5
10	60	0.4	1.5	490	50	467	4.7
11	80	0.3	1.0	398	380	386	3.0
12	80	0.2	1.5	372	350	355	4.5
13	80	0.4	1.0	425	260	450	5.9
14	80	0.3	1.5	444	320	420	5.4
15	100	0.2	1.5	405	550	386	4.7
16	100	0.4	1.5	514	340	544	5.8
17	100	0.3	1.0	412	500	403	2.2
18	80	0.2	0.5	284	900	300	5.6

piece material behaviors under large plastic deformation, high strain rate, and high temperature. According to the JC law, the model for the Von Mises flow stress, σ, is expressed as:

$$\sigma_{eq} = (A + B\varepsilon^n) \cdot \left[1 + C \cdot \ln \frac{\dot{\varepsilon}}{\dot{\varepsilon}_0}\right] \cdot \left[1 - \left(\frac{T - T_{amb}}{T_{fus} - T_{amb}}\right)^m\right] \quad (1)$$

where ε is the equivalent plastic strain, $\dot{\varepsilon}_0$ is the reference strain rate, T_{amb} and T_{fus} are the reference and melting temperature respectively. The five material constants A, B, C, m, n have been already calibrated in Franchi *et al.* [10] by applying an inverse analysis procedure for an orthogonal cutting process in which forces and temperatures were measured. In this work, the temperature is the only physical response studied, see column T_{exp} of Table 3, and the numerical heat transfer coefficient (HTC) is calibrated upon it. The work in Umbrello *et al.* [4] has been followed as a reference.

4. RESULTS

To identify the best range of values some preliminary numerical tests have been performed. Starting from Filice *et al.* [1] a range between 100 (kW/m^2K) and 1000 (kW/m^2K) was chosen. The aim was to get an error, between the measured temperature and the predicted, not exceeding the 6%. It has been seen that the best results were obtained when HTCs values felt between 250 (kW/m^2K) and 500 (kW/m^2K) (for sake of convergence, in some simulations, higher coefficients have been used - even up to a value of 910 (kW/m^2K)). Table 3 shows the numerical heat transfer coefficients, the numerical temperatures associated, and the error percentage between experiment and numerical.

All the coefficients extracted from the simulations have been analysed employing the Exploratory Data Analysis (EDA) techniques. For lack of space not all of them can be shown.

The first step is to examine the sequence/run-order plot of the numerical results. The values are between 50 (kW/m^2K) [the point 10 (60, 0.4, 1.5)] and 910 (kW/m^2K) [the point 5 (100, 0.3, 0.5)]. The lag plot does not show any significant structure, this is also confirmed by the study of correlograms in which no autoregressive behaviour is noticed. The boxplot, the histogram and the density graph show that the response has a Gaussian distribution. The normality plot, see Figure 4, confirms this, as also stated by the Anderson-Darling test which reads a value of about 0.74. Hence, it can be said that the response is normal, without outliers and with independent observations.

Statistical analysis-of-variance provides estimates of the main effects of the factors considered, as well as the joint impacts of factor pairs (2-way interactions). The interaction between 2-factors can be thought as the level of one factor modifying the performance of another. If no interactions are present, the process can be modelled as an additive combination of the factors. When interactions do exist, instead, simple additive models are no longer adequate. However, these interactions can be quantified and included in the model. In this paper, the symbol "x" represents an interaction between two factors. It should not be interpreted as the product of the two factors but as the modifying influence of the factors on each other. Because of the adoption of an orthogonal array, and because of the few numbers of points, limited information about interactions can be provided. Although this, some consideration about the factor pairs will be made in any case. Moreover, when experimenting

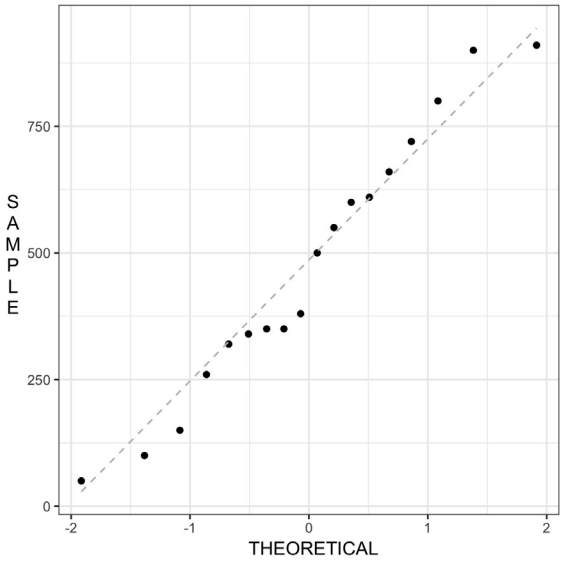

Fig. 4. Normality plot. Anderson-Darling test 0.74

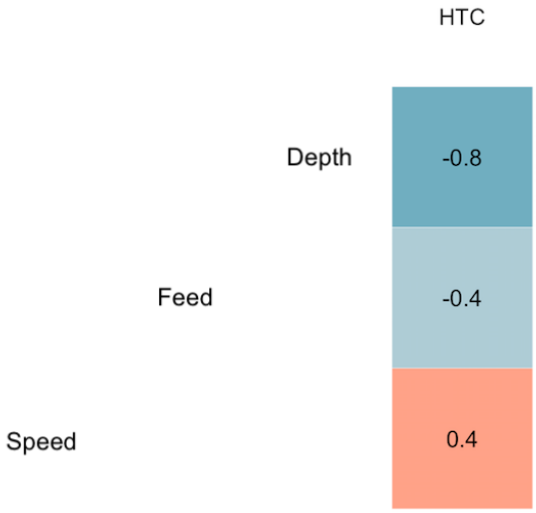

Fig. 5. Matrix correlation plot for the main effects

with only one test for each combination (*i.e.* no-replication), an obvious risk that often occurs is that of modelling randomness. If the response is subject to strong random fluctuations, the no-replicated experiment can lead to misleading conclusions. Non-replicated fractional factorial consists in assuming that certain high-order interactions are negligible and then the sum of their average squares can be used to estimate the error. In few words, the principle of the rarity of the effects is observed: most of the systems are influenced only by some main effects and their low order interactions, while most of the high order interactions are negligible for practical purposes. Following all this, from the matrix of correlations, see Figure 5, the temperature is influenced - in order - by the Depth of Cut (the correlation is 0.8 over 1, high influence), the feed rate (corr = 0.4), and the cutting speed (corr = 0.4). Figure 6 shows the interaction plot: the broken line in the centre of each plot represents the overall av-

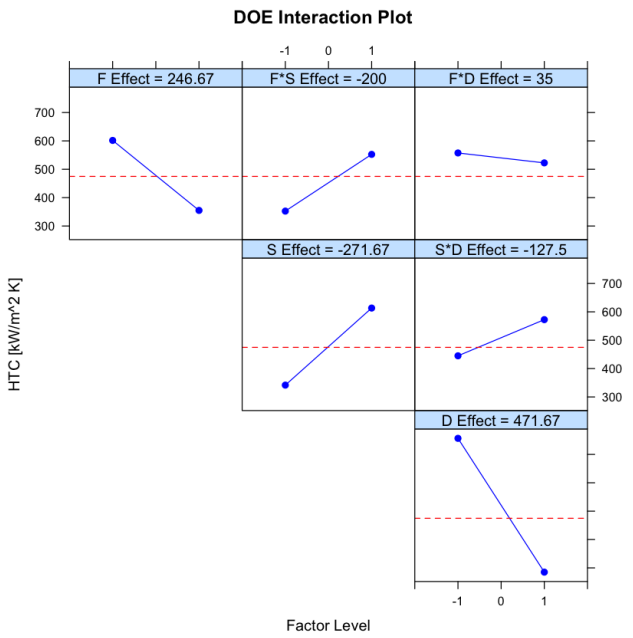

Fig. 6. Interaction plot. The effects were calculated once the factors were coded in -1/0/1 variables. Symbols and Identification following from Table 2

erage of the sensitivity measurements which is 475 (kW/m^2K). The small dots, located on the left and right sides of each plot, represent the average sensitivity, i.e. the low and high levels of the factor respectively. The plots with the largest slopes are associated with the most significant effects. It can be said that the correlation between factors is confirmed and the most important effects, in order, are: D, F, S, F x S, S x D, F x D. With these six terms the used degrees of freedom are already 18, and no ones are free to be used for the error. As said before, in orthogonal designs, conventional analysis of variance methods is not very successful because there are too few degrees of freedom for error. To overcome this fact the inactive effects can be used for this. However, it is not known a-priori, which are the active and inactive effects. A reasonable method for determining the significance of an effect is analysing the half-normal plot, see Figure 7. In this case, since the level for each factor is three, not only the linear but also the quadratic terms have been taken into account. In the end, the terms identified with a significant impact on heat transfer are: $D = D^2$, $S = S^2$, $F = F^2$, F x $D^2 = F^2$ x $D = F^2$ x $D^2 = F$ x D (remembering the confounding).

Based on the significant factors, a regression equation is estimated. Through the Akaike Information Method (AIC) the starting factors are eliminated if they are not significant. Moreover, the mathematical collinearity of the terms F and D is solved through a central transformation, *i.e.* $F_{tr} = (F - F_{mean}) = (F - 0.3)$ and $D_{tr} = (D - D_{mean}) = (D - 1)$. In the end, the regression model obtained reads the following:

$$HTC = -196.8 - 471.6\,D_{tr} + 7.2\,S - 1233.3\,F_{tr} + 737.9\,F_{tr}D_{tr} + 550.0\,D_{tr}^2 + \varepsilon \quad (2)$$

The model has the following performances: R^2 is 99%, the adjusted R^2_{adj} is 98%, the F-Fischer is 322. The residual standard

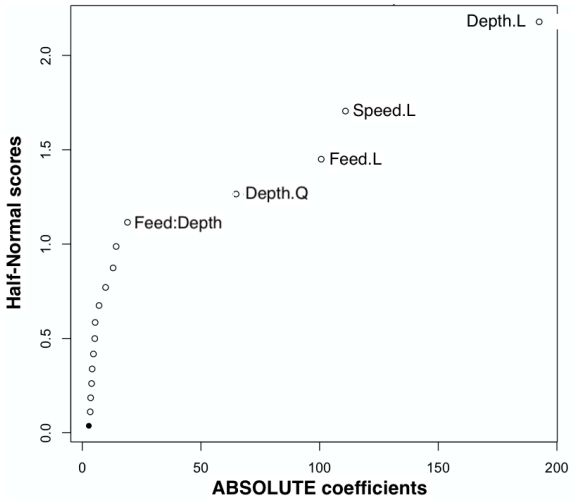

Fig. 7. The linear and quadratic coefficients of the Orthogonal Design

Table 4. Analisi of Variance for the full model

Source	Sum Sq	Df	F value	Pr(> F)
D	743033	2	364.2	<0.0001
S	199511	2	97.8	<0.0001
F	182933	2	89.6	<0.0001
F:D	10711	4	2.6	0.1254
Residuals	7139	7		

Table 5. Predictions compared to sample data

S	F	D	HTC_{prd}	T_{num}	T_{exp}	$\|\Delta\|$ %
100	0.2	0.5	1062	309	326	**5.5**
80	0.2	1.0	507	361	350	**3.0**
60	0.2	1.5	226	347	366	**5.5**
-	-	-	-	-	-	-
40	0.2	0.5	627	246	248	**0.8**
40	0.2	1.0	216	293	305	**4.1**
60	0.1	1.5	312	296	313	**5.7**

error 27, on 12 degrees of freedom, is a measure of the spread of the measurements about their estimated values. The effect plots associated to the model are shown in Figure 8.

Since all the fundamental hypotheses of statistics on the residuals are respected, the ANOVA of the model can be determined, see Table 4.

The equation 2 has been then validated with three experimental points within and three points outside in order to have an independent sample for testing the adequacy of the chosen model. The temperature predictions were obtained by means of the 3D machining model before exploited where the heat transfer coefficients used were predicted by the regression equation 2. The pertinent factor levels, the predicted heat transfer, the predicted and observed temperature, and the error associated with each value are shown in Table 5. All the temperature predictions are under the 6% of error, which is actually a brilliant result. The model is considered validated.

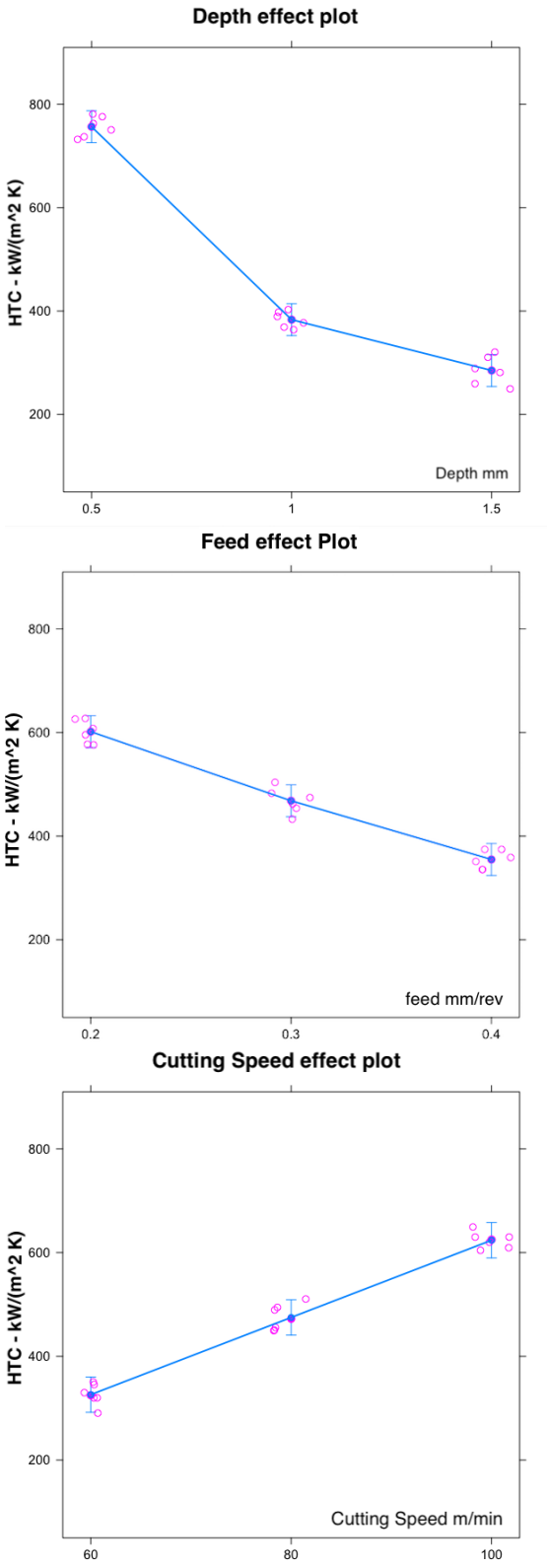

Fig. 8. Effects plots of the regression model

5. CONCLUSION

A strategy has been implemented for the 3D numerical thermal characterization of a dry finish turning for the SAF 2507 stainless steel. The temperature measures, used for the calibration, were acquired by a thermographic tests. The numerical HTCs have been calibrated in order to get numerical temperature results as accurate as possible. The coefficients are influenced firstly by the depth of cut (mostly) and next by the feed rate and cutting speed. Although the samples used to characterize the experimental plan were few, some considerations have been also made for the interactions among factors: i.e. feed/depth interaction is important. In the end, a regression equation for the HTCs is obtained to be used in the numerical model for machining. The methodology has been validated showing very good results.

The strategy here presented has the potential to enable the metal machining community overcoming the challenges involved in the cutting process of super duplex steels. In particular, the industry will directly benefit from this study: in fact, the experiment, the carbide tool, and the super-duplex steel workpiece are coming from an industrial perspective, specifically from the Oil & Gas sector.

6. ACKNOWLEDGMENTS

This work was funded by InnovaPuglia, the inhouse company of the Apulia region, Italy, fostering technological innovation. The funding was the ”Virtual MANufacturing” grant (n. T227BY5) of the Regional Technological Clusters Call.

References

[1] Filice, L., et al. ”On the finite element simulation of thermal phenomena in machining processes.” Advanced Methods in Material Forming. Springer, Berlin, Heidelberg, 2007. 263-278.

[2] Yen, Yung-Chang, et al. ”Estimation of tool wear in orthogonal cutting using the finite element analysis.” Journal of materials processing technology 146.1 (2004): 82-91.

[3] Xie, L-J., et al. ”2D FEM estimate of tool wear in turning operation.” Wear 258.10 (2005): 1479-1490.

[4] Umbrello, D., et al. ”On the evaluation of the global heat transfer coefficient in cutting.” International Journal of Machine Tools and Manufacture 47.11 (2007): 1738-1743.

[5] Burte, Paul R., et al. ”Measurement and analysis of heat transfer and friction during hot forging.” Journal of engineering for industry 112.4 (1990): 332-339.

[6] Childs, T. H. C., K. Maekawa, and P. Maulik. “Effects of Coolant on Temperature Distribution in Metal Machining.” Materials Science and Technology 4.11 (2014): 1006–1019

[7] Grömping, Ulrike. “ R Package DoE.Base for Factorial Experiments .” Journal of Statistical Software 85.5 (2018): n. pag.

[8] Grömping, Ulrike. “Mosaic Plots Are Useful for Visualizing Low-Order Projections of Factorial Designs.” American Statistician 68.2 (2014): 108–116.

[9] Johnson, Gordon R., and William H. Cook. “A Constitutive Model and Data for Metals Subjected to Large Strains, High Strain Rates and High Temperatures.” Proceedings 7th International Symposium on Ballistics (1983): 541–547

[10] Franchi, Rodolfo, Antonio Del Prete, and Domenico Umbrello. “Inverse Analysis Procedure to Determine Flow Stress and Friction Data for Finite Element Modeling of Machining.” International Journal of Material Forming 10.5 (2017): 685–695